5349

Phenylnitrene: Energetics, Vibrational Frequencies, and Molecular Structures

Seung-Joon Kim, Tracy P. Hamilton, and Henry F. Schaefer III*

Contribution from the Center for Computational Quantum Chemistry, University of Georgia, Athens, Georgia 30602. Received September 18, 1991

Abstract: Upon the generation of phenylnitrene (C_6H_5N) by photolysis of phenyl azide, it is possible for the conversion to the cyanocyclopentadienyl radical (C_5H_4CN) or dehydroazepine (seven-membered ring) to take place, depending on experimental conditions. Little is known about the mechanisms or electronic states involved. Characterization of these species by spectroscopic means is difficult because it is frequently unknown which of these intermediates is predominant. For example, a recent analysis of high-resolution electronic spectra leads to the conclusion that the electronic spectrum long attributed to triplet phenylnitrene is due to the cyanocyclopentadienyl radical. This conclusion is supported by the present research. The electronic spectra, vibrational frequencies, and optimized structures (and hence rotational constants) of phenylnitrene are predicted using ab initio quantum chemical techniques, involving double zeta plus polarization (DZP) basis sets and the single and double excitation configuration interaction (CISD) method. The $^3A_2$ state is the ground state, in consensus with all previous work. The theoretical ground-state vibrational frequencies are used to assign the recent experimental IR spectrum for phenylnitrene. The S_0 state is predicted to have the same orbital occupation as T_0; i.e., it is the open-shell singlet $^1A_2$ state. This $^1A_2$ state is 6200 cm^{-1} above T_0 at the highest level of theory but is structurally remarkably different from T_0. The S_1 $^1A_1$ electronic state is qualitatively a superposition of the nitrogen n_x^2 and n_y^2 configurations and is predicted to lie 11 300 cm^{-1} above the T_0 $^3A_2$ ground state. The T_1 state is predicted to be highly puckered with a T_0–T_1 transition energy of 18 600 cm^{-1} and a barrier to planarity of 8000 cm^{-1}.

Introduction

The photochemical reaction of aryl azides has been of interest because of many useful synthetic and industrial applications. It is used in photoaffinity labeling of complex biological mixtures and in making photoresists.[1] Thermolysis or photolysis of the simplest aryl azide, phenyl azide, gives varied products depending on the reaction conditions. The differences in product formation are due to the possibility that one of many highly reactive intermediates may be predominant: phenylnitrene (PhN), dehydroazepine, and the cyanocyclopentadienyl radical. In the early research on this topic, the highly reactive and short-lived intermediate was always assumed to be PhN in either the singlet or the triplet state.

The first report of the electronic spectrum of PhN originates from Reiser et al.'s 1966 work on the photolysis of phenyl azide in an organic matrix at 77 K.[2] Their spectrum is much broader than subsequent gas-phase spectra but clearly shows two relatively well-resolved UV absorptions with maxima at 303 and 368 nm. Since then, several other groups have observed the same UV absorption bands.[3,4] More recently, Leyva et al. investigated the spectra of transient intermediates from the photolysis of phenyl azide in a glassy solution at 77 K and found four separate band systems: around 500, 381, 320, and 240 nm.[5] The first band around 500 nm (which was not reported by Reiser et al.) was assigned to the $n_x \rightarrow \pi^*(a_2)$ and $\pi(a_2) \rightarrow n_x$ transitions in PhN (see Figure 1 for the axis convention used). The other three bands were assigned to $\pi \rightarrow \pi^*$ transitions of triplet PhN based on similarities to the $\pi \rightarrow \pi^*$ excitations in benzyl radicals.

In 1978 Chapman and Le Roux[6] obtained an IR spectrum of an intermediate formed from the photolysis of phenyl azide in an argon matrix at 8 K. With an intense absorption band at 1895 cm^{-1} which is indicative of a strained ketenimine, (normal ketenimines have strong IR absorption bands at 2000 cm^{-1}), they arrived at the conclusion that the predominant intermediate was

the seven-membered ring dehydroazepine. Studies by Schrock and Schuster[7] led them to suggest that this singlet transient, dehydroazepine, is relatively long-lived (in equilibrium with singlet PhN), and that conversion to triplet PhN is slow. The experimental vibrational frequencies for PhN were first reported by Hayes and Sheridan[8] in 1990 from the IR spectrum of a mixture of dehydroazepine and PhN in low-temperature matrices.

Turning to gas-phase studies of PhN, a UV absorption band at 368.3 nm which was observed in the flash photolysis of *o*-chloroaniline and phenyl isocyanate by Porter and Ward[9] was assigned to triplet PhN in 1968. With the low-temperature matrix isolation spectrum around 368 nm,[2] the gas-phase assignment was accepted and reproduced by several groups.[10–12]

Very recently Cullin and co-workers[13] found that the rotational and spin structure of the UV band attributed to triplet PhN in the gas phase is inconsistent with the expected geometric and spin structure of PhN. The cyanocyclopentadienyl radical was suggested as an alternative candidate for the gas-phase intermediate, and this hypothesis was confirmed by a subsequent paper[14] that further investigated that possibility. Their main conclusion is that the electronic spectrum of PhN in the gas phase has not yet been detected, but that the condensed phase carrier could still be PhN.

An experimental triplet–singlet splitting of 4.3 kcal/mol in PhN was first obtained from the photodetachment spectra for the PhN anion by Drzaic and Brauman.[15,16] Ozawa and co-workers[12] subsequently performed laser-induced fluorescence (LIF) experiments on gas-phase products of phenyl azide photolysis, and assigned the peak shifted by 2202 cm^{-1} from the 0–0 band as the T_1–S_0 electronic transition of PhN, resulting in a T_0–S_0 gap of 6.3 kcal/mol. However, they rejected their previous assignment

(1) Scriven, E. F. V. *Azides and Nitrenes (Reactivity and Utility)*; Academic Press: New York, 1984.
(2) Reiser, A.; Bowes, G.; Horne, P. J. *Trans. Faraday Soc.* **1966**, *62*, 3162.
(3) Smirnov, V. A.; Brichkin, S. B. *Chem. Phys. Lett.* **1982**, *87*, 548.
(4) Feilchenfeld, N. B.; Waddell, W. H. *Chem. Phys. Lett.* **1983**, *98*, 190.
(5) Leyva, E.; Platz, M. S.; Persy, G.; Wirz, J. *J. Am. Chem. Soc.* **1986**, *108*, 3783.
(6) Chapman, O. L.; Le Roux, J. P. *J. Am. Chem. Soc.* **1978**, *100*, 282.

(7) Schrock, A. K.; Schuster, G. B. *J. Am. Chem. Soc.* **1984**, *106*, 5228.
(8) Hayes, J. C.; Sheridan, R. S. *J. Am. Chem. Soc.* **1990**, *112*, 5879.
(9) Porter, G.; Ward, B. *Proc. R. Soc. London* **1968**, *A303*, 139.
(10) Lehman, P. A.; Berry, R. S. *J. Am. Chem. Soc.* **1973**, *95*, 8614.
(11) Hancock, G.; McKendrick, K. G. *J. Chem. Soc., Faraday Trans.* **1987**, *83*, 2011.
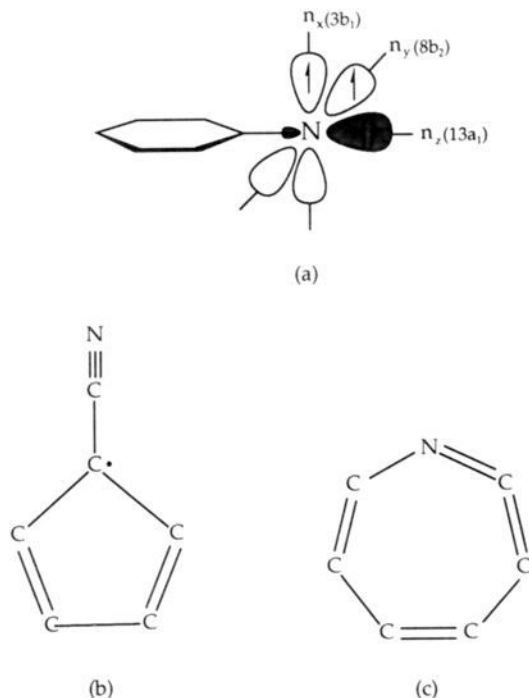(12) Ozawa, K.; Ishida, T.; Fuke, K.; Kaya, K. *Chem. Phys. Lett.* **1988**, *150*, 249.
(13) Cullin, D. W.; Yu, L.; Williamson, J. M.; Platz, M. S.; Miller, T. A. *J. Phys. Chem.* **1990**, *94*, 3387.
(14) Cullin, D. W.; Soundararajan, N.; Platz, M. S.; Miller, T. A. *J. Phys. Chem.* **1990**, *94*, 8890.
(15) Drzaic, P. S.; Brauman, J. I. *J. Am. Chem. Soc.* **1984**, *106*, 3443.
(16) Drzaic, P. S.; Brauman, J. I. *J. Phys. Chem.* **1984**, *88*, 5285.

(a)

(b)   (c)

Figure 1. The structure of three intermediates commonly seen in the photolysis of phenyl azide: (a) phenylnitrene; (b) cyanocyclopentadienyl radical; and (c) dehydroazepine. The Cartesian coordinate axis system used for phenylnitrene is shown, along with the nonbonding nitrogen orbitals associated with the ground-state occupation.

in a more recent paper[17] because their unpublished ab initio calculations predicted that the lowest singlet state was located approximately 30 kcal/mol above the ground-state triplet. The other reason for their reassignment is that they observed the same spectrum in the excimer laser photolysis of cyanocyclopentadiene (C_5H_5CN). These findings led them to assign this spectrum to the C_5H_4CN radical instead of PhN.

In light of these recent laboratory revelations about PhN, an ab initio investigation is warranted. In this paper we report the vibrational frequencies, the ground-state structure (and rotational constants), and vertical and adiabatic excitation energies with particular emphasis on the T_0–S_0 and T_0–T_1 energy gaps. Separate studies on the cyanocyclopentadienyl radical system are planned, but preliminary results will be briefly discussed. The vibrational frequencies will be compared with the IR spectrum presented by Hayes and Sheridan,[8] and the electronic spectrum will be contrasted with the gas-phase UV–visible spectrum that was assigned to PhN until recently and with the low-temperature matrix UV–visible spectrum. The rotational constants will be examined for similarities to or differences from those measured by Cullin et al.[13,14]

Theoretical Approach

The three basis sets used in this work were of double zeta (DZ), DZ+d, and double zeta plus polarization (DZP) quality. The DZ basis is the standard Huzinaga–Dunning[18,19] (9s5p/4s2p) contracted basis set for carbon and nitrogen, and the (4s/2s) set for hydrogen. The DZ+d basis was obtained from the DZ basis by adding a single set of polarization functions (six-component d-like functions) on carbon and nitrogen with $\alpha_d(C) = 0.75$, $\alpha_d(N) = 0.80$. The third basis, DZP, consisted of the DZ+d basis with a set of polarization p functions on each hydrogen with $\alpha_p(H) = 0.75$.

The optimized geometries for the ground-state triplet ($^3A_2$), first excited (open-shell) singlet ($^1A_2$), excited triplets ($^3A_1$, $^3B_1$,

$^3B_2$), and two other closed-shell singlet ($^1A_1$) configurations for PhN were obtained by analytic gradient techniques[20] with the DZ, DZ+d, and DZP basis sets at the SCF level of theory. Since the two closed-shell configurations lie in close proximity energetically, the two-configuration (TC) SCF method was used to describe the lower state arising from these two electron configurations. A full geometrical optimization of the lowest $^1A_1$ state was carried out using analytic TCSCF gradient methods. At this equilibrium geometry the coefficients of the two configurations are 0.889 ($8b_2^2$) and −0.458 ($3b_1^2$).

For the $^3A_2$, $^3B_1$, and $^1A_2$ states, the geometries were optimized at the single and double excited configuration interaction (CISD) level with the DZ+d basis set by employing analytic CISD gradient methods.[21] Seven frozen core and seven deleted virtual molecular orbitals were used in CISD optimizations. The CISD energies were corrected for unlinked quadruple excitations by using Davidson's method; the corrected CISD will be denoted by CISD+Q.[22] For the $^3B_1$ T_1 state in C_s symmetry, the CISD wave function consisted of 677 986 configuration-state functions. For the lowest $^1A_1$ state, a two-reference DZ+d CISD wave function was determined at the DZ+d TCSCF equilibrium geometry. The appropriate two-reference Davidson correction was applied to the total energy of this $^1A_1$ state.

The harmonic vibrational frequencies and infrared intensities for all of the above states were evaluated via analytic second energy derivatives[23] at the SCF level with the DZ and DZ+d bases, but only the DZ+d SCF results are reported.

The vertical excitation energies from the ground state to various excited singlet and triplet states were also obtained using the DZ+d CISD energies computed at the optimized DZ+d CISD geometry of the ground state. The adiabatic excitation energies were evaluated from the energy differences between their optimized minima at the DZ+d CISD level, and included zero-point vibrational energy (ZPVE) corrections for the T_0 and excited states computed from their respective DZ+d SCF harmonic frequencies. The ZPVE corrections were obtained by scaling the harmonic frequencies by a factor of 0.91 as advocated by Grev et al.,[24] who expound on the difference between the scaling factor needed to reproduce ZPVEs and the optimum scaling factor for fundamental frequencies.

Results and Discussion

The main thrust of this research is to predict the spectral features of PhN. The electronic configurations for the 12 states investigated in this work are as follows:

...$(13a_1)^2(2b_1)^2(1a_2)^2(8b_2)(3b_1)$	$^3A_2$ (T_0) and $^1A_2$ (S_0)	
...$(13a_1)^2(2b_1)^2(1a_2)^2(8b_2)^2$	$^1A_1$ (S_1)	$n_x(3b_1) \rightarrow n_y(8b_2)$
...$(13a_1)^2(2b_1)^2(1a_2)^2(3b_1)^2$	$^1A_1$ (S_2)	$n_y(8b_2) \rightarrow n_x(3b_1)$
...$(13a_1)^2(2b_1)^2(1a_2)(8b_2)(3b_1)^2$	$^3B_1$ (T_1)	$\pi_3(1a_2) \rightarrow n_x(3b_1)$
...$(13a_1)(2b_1)^2(1a_2)^2(8b_2)(3b_1)^2$	$^3B_2$ (T_2)	$n_z(13a_1) \rightarrow n_x(3b_1)$
...$(13a_1)(2b_1)^2(1a_2)^2(8b_2)^2(3b_1)$	$^3B_1$ (T_3)	$n_z(13a_1) \rightarrow n_y(8b_2)$
...$(13a_1)^2(2b_1)(1a_2)^2(8b_2)^2(3b_1)$	$^3A_1$ (T_4)	$\pi_2(2b_1) \rightarrow n_y(8b_2)$
...$(13a_1)^2(2b_1)^2(1a_2)(8b_2)^2(3b_1)$	$^3B_2$ (T_5)	$\pi_3(1a_2) \rightarrow n_y(8b_2)$
...$(13a_1)^2(2b_1)^2(1a_2)^2(8b_2)(2a_2)$	$^3B_1$ (T_6)	$n_x(3b_1) \rightarrow \pi_1^*(2a_2)$
...$(13a_1)^2(2b_1)^2(1a_2)^2(3b_1)(4b_1)$	$^3A_1$ (T_7)	$n_y(8b_2) \rightarrow \pi_2^*(4b_1)$
...$(13a_1)^2(2b_1)^2(1a_2)^2(3b_1)(2a_2)$	$^3B_2$ (T_8)	$n_y(8b_2) \rightarrow \pi_1^*(2a_2)$

The labeling (e.g., T_4) of the electronic states in this paper is not meant to imply a definite energetic ordering. To cite just one example, there may be two more triplet states ($^3A_2$) between T_1 and T_8. One is reached by the $\pi_2 \rightarrow n_x$ transition to the electronic state with the configuration ...$(13a_1)^2(2b_1)(1a_2)^2(8b_2)(3b_1)^2$.

(17) Ishida, T.; Abe, H.; Nakajima, A.; Kaya, K. *Chem. Phys. Lett.* **1990**, *170*, 425.
(18) Huzinaga, S. *J. Chem. Phys.* **1965**, *42*, 1293.
(19) Dunning, T. H. *J. Chem. Phys.* **1970**, *53*, 2823.

(20) Pulay, P. In *Modern Theoretical Chemistry*; Schaefer, H. F., Ed.; Plenum: New York, 1977; Vol. 4, p 153. Goddard, J. D.; Handy, N. C.; Schaefer, H. F. *J. Chem. Phys.* **1979**, *71*, 1525.
(21) Brooks, B. R.; Laidig, W. D.; Saxe, P.; Goddard, J. D.; Yamaguchi, Y.; Schaefer, H. F. *J. Chem. Phys.* **1980**, *72*, 4652.
(22) Langhoff, S. R.; Davidson, E. R. *Int. J. Quantum Chem.* **1974**, *8*, 61.
(23) Saxe, P.; Yamaguchi, Y.; Schaefer, H. F. *J. Chem. Phys.* **1982**, *77*, 5647.
(24) Grev, R. S.; Janssen, C. L.; Schaefer, H. F. *J. Chem. Phys.* **1991**, *95*, 5128.

Phenylnitrene

J. Am. Chem. Soc., Vol. 114, No. 13, 1992 5351

Table I. Absolute and Adiabatic Excitation Energies for Several States of Phenylnitrene at Various Levels of Theory[a]

states	DZ SCF	DZ+d SCF	DZ+d CISD	DZ+d CISD+Q
absolute energy (hartrees)				
$^3A_2$ (T_0)	−284.443 01	−284.550 64	−285.264 56	−285.390 41
$^1A_2$ (S_0)	−284.389 97	−284.511 08	−285.232 58	−285.361 29
$^1A_1$ (S_1, TCSCF/TC-CISD)	−284.383 47	−284.493 30	[−285.212 09]	[−285.338 77]
$^1A_1$ (S_1)	−284.369 16	−284.481 72	[−285.204 70]	[−285.333 05]
$^1A_1$ (S_2)	−284.344 54*	−284.456 37*	[−285.177 88]*	[−285.306 28]*
$^3B_1$(T_1) nonplanar	−284.309 11	−284.439 89	−285.172 23	−285.303 94
$^3B_1$(T_1) planar	−284.288 20	−284.411 56	−285.136 70	−285.267 31
$^3B_2$ (T_2)	−284.302 24	−284.405 80	−285.116 40	−285.241 75
$^3B_1$ (T_3)	−284.301 71*	−284.403 96*		
$^3A_1$ (T_4)	−284.277 41	−284.400 31		
$^3B_2$ (T_5)	−284.263 06*	−284.385 97*		
$^3B_1$ (T_6)	−284.246 60*	−284.367 68*		
$^3A_1$ (T_7)	−284.224 56*	−284.336 85*		
$^3B_2$ (T_8)	−284.199 63*	−284.322 08*		
adiabatic excitation energy (cm⁻¹)				
$T_0 - S_0$	11 600 (11 400)	8 700 (8 500)	7 000 (6 800)	6 400 (6 200)
$T_0 - T_1$	29 400 (29 000)	24 300 (23 900)	20 300 (19 800)	19 000 (18 600)
$T_0 - T_2$	30 900 (30 700)	31 800 (31 600)	32 500 (32 400)	32 600 (32 500)

[a] CISD total energies in brackets were evaluated at the corresponding SCF or TCSCF equilibrium geometries. All other CI results involved full CI geometry optimizations. Note that energies indicated by asterisks are not true upper bounds to the energies of the electronic states in question. The results in parentheses include the zero-point vibrational energy (ZPVE) correction. For all corrections, the DZ+d SCF frequencies are used and scaled by a factor of 0.91.[24]

Table II. Vertical Excitation Energies (cm⁻¹) from the Ground State ($^3A_2$) to Various Excited States at the DZ+d CISD Level of Theory

states	DZ+d CISD	DZ+d CISD+Q
$T_0 - S_0$	10 900	10 400
$T_0 - S_1$	13 800	13 200
$T_0 - T_1$	32 200	31 200
$T_0 - T_2$	32 800	33 000
$T_0 - T_4$	36 700	36 700

Efforts to compute that wave function invariably resulted in the T_0 wave function. The state arising from a $n_x \rightarrow \pi_2^*$ transition also leads to a state for which obtaining a wave function is intractable. These computationally inaccessible states should be near the so-called T_1 and T_6 states. For all other excited triplet states except the T_1 and T_2 state, optimizations past the DZ+d SCF level of theory were not performed. Thus, the DZ+d SCF method is used to conveniently label the electronic states, even though we know that such an energetic ordering will often be wrong.

From analyzing the molecular orbitals for the $^3A_2$ ground state, we found that the two singly occupied orbitals, $8b_2$ and $3b_1$, correspond to an in-plane p_y orbital and an out-of-plane p_x orbital on the nitrogen atom, respectively. The p_x orbital on nitrogen is (by convention) perpendicular to the phenyl ring and is in conjugation with the ring π system. The two highest doubly occupied orbitals, $2b_1$ and $1a_2$, are the higher two of the three ring π orbitals and $13a_1$ is the lone pair p_z orbital on nitrogen. In the discussion to follow, $13a_1$ is called the n_z orbital, $2b_1$ and $1a_2$ are named π_2 and π_3, $8b_2$ and $3b_1$ are denoted by n_y and n_x, and $2a_2$ and $4b_1$ are called π_1^* and π_2^*. Table I gives absolute energies for the above states, and some adiabatic excitation energies at various levels of theory. Table II presents the vertical excitation energies at the DZ+d CISD and DZ+d CISD+Q levels of theory. The DZP SCF results are not presented here because they are very similar to the DZ+d SCF values, and we report correlated results with the DZ+d basis. As shown in Table I, the $^3A_2$ state is confirmed in our study to be the ground state, T_0. This was previously thought to be the case based on the parent molecule NH which has a $^3\Sigma^-$ ground state. The ground state generally remains as a triplet upon aryl or alkyl substitution.[9]

Excitation Energies

In order to find the lowest excited triplet state for PhN, we explored many possible low-lying triplet states. The $^3B_1$ state with the electronic configuration of $...(13a_1)^2(2b_1)^2(1a_2)(8b_2)(3b_1)^2$ turns out to be the T_1 state. This state is the result of a one electron excitation from the ring π_3 orbital (the highest doubly occupied

orbital) to the n_x (higher singly occupied) orbital on nitrogen. The predicted T_0-T_1 adiabatic transition energies decrease smoothly as higher levels of theory are employed. The DZ+d CISD+Q adiabatic transition of 18 600 cm⁻¹ corresponds to a UV band at 539 nm. This result is in good agreement with the UV bands observed by Leyva et al. around 500 nm in a glassy solution at 77 K.[5] They assigned these bands to the $n_x \rightarrow \pi_1^*$ transition (which leads to our T_6 state) and to the $\pi_3 \rightarrow n_x$ excitation which is, in fact, the T_0-T_1 transition. This is in contrast to the earlier belief that the bands around 370 nm in the gas and matrix isolation UV–visible spectra were the T_0-T_1 bands due to a $\pi \rightarrow \pi^*$ transition.[2]

The T_0-T_1 transition is allowed by symmetry, but is complicated by the fact that T_1 is predicted to be puckered, with a DZ+d SCF barrier to planarity of 6200 cm⁻¹. The DZ+d CISD barrier is 7800 cm⁻¹ and the DZ+d CISD+Q barrier is 8000 cm⁻¹. The 368-nm band of Reiser et al. is between the vertical excitation energy of 31 150 cm⁻¹ (321 nm), and the adiabatic value of 539 nm. The above differences in the SCF and CISD barriers demonstrate that electron correlation is clearly needed to describe the energy difference between states with differing occupations of π electrons. Excitation out of a π orbital makes the planar conformation less stable. It is not unusual for low-lying excited states to exhibit these types of distortions in molecules with π bonds. For example, the lowest excited state of formaldehyde is pyramidal and the lowest excited state of acetylene is bent.

A $^3B_2$ state is the second excited triplet state, T_2, accessed by a $n_z \rightarrow n_x$ transition. The reason for the higher energy in the $n_z \rightarrow n_x$ transition (T_2) than in the $\pi_3 \rightarrow n_x$ transition (T_1) can be explained by the energetically deep nonbonding n_z orbital on nitrogen relative to the ring π orbitals (π_2, π_3). The T_0 and T_2 states are equally well described at the SCF and CISD levels; therefore, the predicted adiabatic transition energies are nearly constant. The small effect of the Davidson correction on the T_0-T_2 vertical excitation energy is consistent with the supposition that T_0 and T_2 are equally well described with or without correlation. This is in contrast to the 1000-cm⁻¹ effect of the Davidson correction for the T_0-T_1 energy difference.

The third excited triplet state (at the DZ+d SCF level) corresponds to $n_z \rightarrow n_y$ transition. The T_3 state is very close to the T_2 state, namely, 400 cm⁻¹ (1.1 kcal/mol) higher than the T_2 state at the DZ+d SCF level. However, this order of T_2 and T_3 is to be expected since conjugation stabilizes the electronic configuration of T_2, which has two electrons in the n_x orbital instead of one electron in the n_x orbital for T_3. There is evidently less interaction between n_x and the ring π orbitals for the T_2 and T_3 states than for T_1.
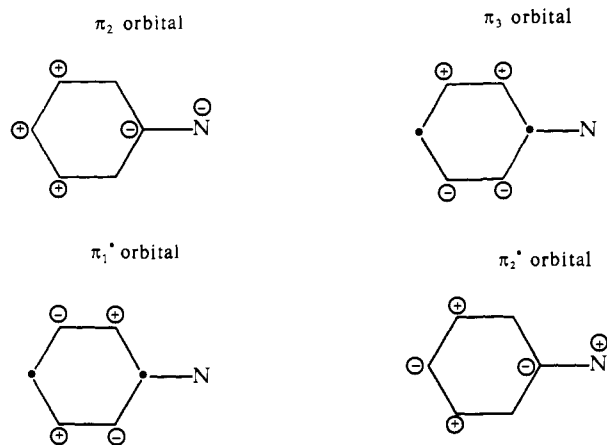
Figure 2. The highest two bonding and lowest two antibonding π orbitals of $^3A_2$ ground state of phenylnitrene.

There are two $\pi \rightarrow n_y$ transitions which lead to the T_4 and T_5 electronic states. A one-electron transition from the π_2 to the n_y orbital gives the T_4 state of $^3A_1$ symmetry. Electronic excitation to this $^3A_1$ state from the $^3A_2$ ground state is forbidden by symmetry. The T_4 state lies 800 cm^{-1} above the T_3 state at the DZ+d SCF level. The order of T_4 and T_5 is the opposite of one which is expected since π_3 is higher than π_2. This is probably because the interaction of the singly occupied π_2 orbital with the half-occupied n_x orbital is more favorable than the interaction of n_x and π_3 which has a node at nitrogen (see Figure 2).

The next excited triplet state considered here, designated T_6, is the $^3B_1$ state reached by a $n_x \rightarrow \pi_1^*$ transition. This transition was previously thought to be the source of the 368.3-nm band in the electronic spectrum for which PhN was believed to be the carrier.[11] The adiabatic transition energy between the T_0 and T_6 states is 39 200 cm^{-1} (255 nm) at the DZ+d SCF level. However, this result can not be taken seriously, because the state we have labeled T_6 is energetically the third state of $^3B_1$ symmetry. A proper theoretical treatment of the state labeled T_6 would require the third energy eigenvalue of $^3B_1$ symmetry. The $n_x \rightarrow \pi_2^*$ transition was not amenable to study, as mentioned above, but should be in the vicinity of T_6.

There are two $n_y \rightarrow \pi^*$ transitions which lead to relatively high-lying states, T_7 and T_8. The adiabatic energy gap from the ground state to the T_7 state is 46 900 cm^{-1} at the DZ+d SCF level. Surprisingly, excitation of an electron from n_y to π_1^* to give the T_8 state is 3200 cm^{-1} above the transition to the T_7 state via $n_y \rightarrow \pi_2^*$ excitation at the same level of theory. The same argument for the reverse order of T_4 and T_5 applies here except that π^* orbitals are involved instead of π orbitals. The π_2^* orbital can interact with the singly occupied n_x orbital, whereas π_1^* has a node at nitrogen.

The lowest singlet state, S_0, for PhN is the *open-shell* $^1A_2$ state which has the same electronic configuration as the ground state but antiparallel spins for the two unpaired electrons. The S_0 state is predicted to lie 6200 cm^{-1} (17.7 kcal/mol) above the ground state at the DZ+d CISD+Q level. This is far from the previous experimental values of 4.3 kcal/mol (1500 cm^{-1})[15,16] and 2202 cm^{-1}[12] once deduced for PhN. The latter feature was reassigned to the C–N stretching frequency of C_5H_4CN by Ishida et al. when they found that the S_0 state was located 10 000 cm^{-1} above the T_0 state from their unpublished ab initio calculations.[17] Their number is consistent with our SCF values, and is probably an SCF result also, although not explicitly identified as such. The T_0–S_0 excitation energies decrease as higher levels of theory are used because electron correlation typically lowers the energies of the singlet states compared to the triplets.

Comparing PhN with the related molecules NH and CH$_3$N, we find that the singlet–triplet energy separation of 17.7 kcal/mol in PhN is relatively small. At the DZ+d CISD+Q level, the S–T energy gaps for NH and CH$_3$N are 42.2 and 38.2 kcal/mol. The experimental $\tilde{X}^3\Sigma^-$ – $a^1\Delta$ energy difference of NH is 36 kcal/mol.

The large difference between theoretical and experimental values for the S–T energy gap of NH is surprising. However, even at a high level of theory (MCSCF-CI with 11s7p2d/7s2p basis set), the theoretical S–T splitting for NH is 40.6 kcal/mol.[25] Our S–T separation for CH$_3$N is nearly identical with the value of 38.6 kcal/mol at the DZP CISD+Q level.[26] Both of these molecules have ground states that are triplets, and both have open-shell singlets for the S_0 states.[26,27] On examining the molecular orbitals for the S_0 state of PhN, we find that there is a very large mixing between the π-type p_x orbital (n_x) on nitrogen and the bonding π orbital of appropriate symmetry in the ring. This large coupling stabilizes the S_0 state, decreasing the S–T energy separation in PhN relative to NH and CH$_3$N. As a matter of fact, the π_2 and n_x orbitals (with b_1 symmetry) for S_0 are remarkably changed from those of T_0.

The next two excited singlet states, S_1 and S_2, for PhN are closed-shell singlets. The larger electron–electron repulsion between the two electrons in the closed shells make them slightly higher in energy than the open-shell singlet (S_0) state. The DZ+d SCF adiabatic energy difference $S_0 - S_1$ is 6400 cm^{-1}, which energy difference does not include a ZPVE correction. With the more appropriate TCSCF description of the S_1 state, its energy with respect to S_0 is 3900 cm^{-1}. The DZ+d TC-CISD energy similarly lies 4500 cm^{-1} above the DZ+d CISD energy for the S_0 $^1A_2$ state. Note that in the TC-CISD wave function the lead coefficients are 0.820 ($8b_2^2 = n_y^2$) and -0.388 ($3b_1^2 = n_x^2$). Finally the DZ+d Davidson-corrected TC-CISD treatment places the S_1 state 4900 cm^{-1} higher than S_0 $^1A_2$. The b_1 orbitals in the S_1 and S_2 states resemble the S_0 orbitals much more than they resemble the T_0 orbitals. CISD optimizations were not performed for these higher-lying singlet states.

Vibrational Frequencies

The first measurement of the IR spectrum for PhN in the range of 654–1552 cm^{-1} was reported without detailed assignments for each peak by Hayes and Sheridan[8] in 1990. The DZ+d SCF harmonic vibrational frequencies for the T_0 state at its optimized equilibrium geometry are listed in Table III. When comparing the theoretical and experimental frequencies, it is important to remember that such SCF frequencies are typically 10% high. There are no vibrational frequencies in the range of 1800–3000 cm^{-1} for the ground state of PhN, implying that the strong band located near 2200 cm^{-1} to the red of the 368-nm band[12,14] should not be assigned to any fundamental vibrational frequency of PhN.

There are three IR inactive a_2 modes among the 30 vibrational frequencies for the ground state of PhN (which has C_{2v} symmetry). The observed frequency of 746 cm^{-1} with the strongest intensity compares favorably with the theoretical value of 839 cm^{-1} which has the highest predicted intensity and is assigned to the CH out-of-plane bending mode. The CN stretch frequency of 1345 cm^{-1} for the ground state of PhN matches with the experimental value of 1287 cm^{-1}, which is similar to the experimental value of 1276 cm^{-1} in aniline.[28] These C–N stretching frequencies are significantly higher than the C–N stretch of 1039 cm^{-1} in triplet ground state CH$_3$N from experiment.[29] The CN stretching mode in phenylnitrene is strongly coupled with the ring stretching modes, as are some of the CH in-plane bending modes. This mode mixing makes definite individual assignments difficult. The other probable assignments for the experimental frequencies of PhN are shown in Table III. The observed frequencies[8] of 1497, 1309, and 1408 cm^{-1} are assigned to the overtones and to the combination band of the 746- and 654-cm^{-1} fundamentals. The remaining assignments for experimental frequencies are more tentative.

Table III also gives the experimental vibrational frequencies for the related aniline molecule PhNH$_2$, except for the N–H

(25) Alexander, M. H.; Werner, H.-J.; Dagdigian, P. J. *J. Chem. Phys.* **1988**, *89*, 1388.

(26) Demuynck, J.; Fox, D. J.; Yamaguchi, Y.; Schaefer, H. F. *J. Am. Chem. Soc.* **1980**, *102*, 6204.

(27) Yarkony, D. R.; Schaefer, H. F.; Rothenberg, S. *J. Am. Chem. Soc.* **1974**, *96*, 5974.

(28) Evans, J. C. *Spectrochim. Acta*, **1960**, *16*, 428.

(29) Carrick, P. G.; Engelking, P. C. *J. Chem. Phys.* **1984**, *81*, 1661.

Table III. Harmonic Vibrational Frequencies ω″ (cm⁻¹) and Infrared Intensities I (km/mol) for the Ground State of PhN at the DZ+d SCF Level

	mode description	sym	PhN (T_0) theory ω″ (I)	PhN (T_0) expt[a] ω″ (rel I)	aniline expt[b] ω″
1	CH stretch	a_1	3409 (14)		3072
2	CH stretch	b_2	3403 (33)		3088
3	CH stretch	a_1	3394 (16)		3053
4	CH stretch	b_2	3386 (2)		3025
5	CH stretch	a_1	3377 (0)		3037
6	ring stretch	a_1	1784 (1)		1603
7	ring stretch	b_2	1761 (4)		1590
8	CH bend (in) + ring str	a_1	1641 (7)	1552 (0.68)	1503
9	CH bend (in) + ring str	b_2	1586 (3)	1524 (0.33)	1468
10	CH bend (in)	b_2	1443 (0)		1324[c]
11	CN stretch	a_1	1345 (8)	1287 (0.47)	1276
12	CH bend (in) + ring str	b_2	1324 (2)	1286 (0.49)	1190[c]
13	CH bend (in)	a_1	1275 (1)		1173
14	ring str	b_2	1197 (5)	1148 (0.32)	1152
15	ring str	b_2	1163 (3)	1079 (0.22)	1090
16	ring str + CH bend (in)	a_1	1114 (3)	1008 (0.17)	1028
17	CH bend (out)	b_1	1113 (0)		968
18	CH bend (out)	a_2	1096 (0)		957
19	ring bend (in) + ring str	a_1	1077 (0)		990
20	CH bend (out)	b_1	1031 (6)	964 (0.06)	874
21	CH bend (out)	a_2	944 (0)		825
22	ring stretch + CN str	a_1	880 (0)		812
23	CH bend (out)	b_1	839 (90)	746 (1.00)	745
24	ring torsion	b_1	757 (31)	654 (0.55)	690
25	ring bend (in)	b_2	667 (0)		619
26	ring bend (in)	a_1	561 (0)		526
27	CN bend (out)	b_1	532 (4)		500
28	ring torsion	a_2	447 (0)		415
29	CN bend (in)	b_2	395 (6)		390
30	ring torsion	b_1	252 (1)		233

[a] Reference 8. [b] Reference 28. [c] These are based on the modified assignments by Niu et al.[30]

stretches and bends which have no counterpart in PhN. These values were reported originally by Evans,[28] but the modified assignment of Niu et al.[30] is shown. A comparison of our PhN frequencies with those of aniline shows similarities after reducing the SCF frequencies by 10%. There are a few ambiguities in matching the assignments for PhN and PhNH₂, again because of the difficulty of the definite individual assignments caused by mode coupling. In the range of 1000–1600 cm⁻¹ for the observed frequencies, ring stretching modes and in-plane CH bending modes are significantly coupled to make independent assignment difficult for both PhN and aniline. For instance, the ν_8 and ν_9 vibrations in aniline are mainly ring stretches with some in-plane CH bending, but these modes are assigned to in-plane CH bending coupled with some ring stretching for PhN. The only difference in the order of the assigned frequencies for PhN and aniline is that the observed frequency of 990 cm⁻¹ assigned to ring breathing in aniline is higher than the highest out-of-plane CH bend mode. However, in PhN this same mode occurs at a frequency below the second out-of-plane CH bending and is assigned to a mode that is primarily in-plane ring bending coupled to ring stretching.

The assignments for the vibrational frequencies of the S_0 state are shown in Table IV. The S_0 state has a planar structure and C_{2v} symmetry like the ground state. However, the vibrational frequencies for the planar structure of the T_1 state of PhN include one imaginary frequency, which means that this state is not a minimum but a transition state. A puckered structure with C_s symmetry for the T_1 state is the minimum at the DZ+d SCF and CISD level. The assignment of each frequency to a unique internal coordinate is also very difficult for these two states.

The vibrational frequency for the C–N stretch in PhN increases from 1345 cm⁻¹ in the ground state to 1855 cm⁻¹ in the S_0 state. This result reflects the fact that the C–N bond length is shorter in the S_0 state than in the ground state (see Figure 3 and Table V). The S_0 ring torsion modes (puckering) are consistently lower in frequency than those of T_0.

(30) Niu, Z.; Dunn, K. M.; Boggs, J. E. *Mol. Phys.* **1985**, *55*, 421.

Table IV. Harmonic Vibrational Frequencies ω′ (cm⁻¹) and Infrared Intensities I (km/mol) for the S_0 State of PhN at the DZ+d SCF Level

	mode description	sym	S_0 ω′ (I)
1	CH stretch	a_1	3422 (12)
2	CH stretch	b_2	3416 (18)
3	CH stretch	a_1	3412 (7)
4	CH stretch	b_2	3388 (12)
5	CH stretch	a_1	3384 (3)
6	CN stretch	a_1	1855 (63)
7	ring stretch	b_2	1722 (0)
8	ring stretch	a_1	1722 (15)
9	ring str + CH bend (in)	b_2	1551 (5)
10	CH bend (in)	b_2	1537 (11)
11	CH bend (in) + ring str	a_1	1484 (1)
12	CH bend (in) + ring str	b_2	1362 (5)
13	CH bend (in) + ring str	a_1	1278 (1)
14	CH bend (in)	b_2	1238 (6)
15	ring str + CH bend (in)	b_2	1136 (4)
16	CH bend (out)	a_1	1094 (0)
17	CH bend (out)	b_1	1088 (0)
18	ring bend (in)	a_2	1048 (0)
19	ring stretch	a_1	960 (0)
20	CH bend (out)	b_1	918 (57)
21	CH bend (out)	a_2	837 (0)
22	ring stretch	a_1	834 (0)
23	ring tors + CH bend (out)	b_1	768 (7)
24	CH bend (out)	b_1	634 (58)
25	ring bend (in)	b_2	624 (0)
26	ring bend (in)	a_1	540 (3)
27	ring tors + CN bend (out)	b_1	454 (1)
28	CN bend (in)	a_2	427 (15)
29	ring torsion	b_2	425 (0)
30	ring torsion	b_1	161 (3)

Geometries

The optimized geometries for the ground state of PhN at various levels of theory are shown in Figure 3. The C–N bond length is 1.402 Å at the DZ+d SCF level and CISD decreases this to
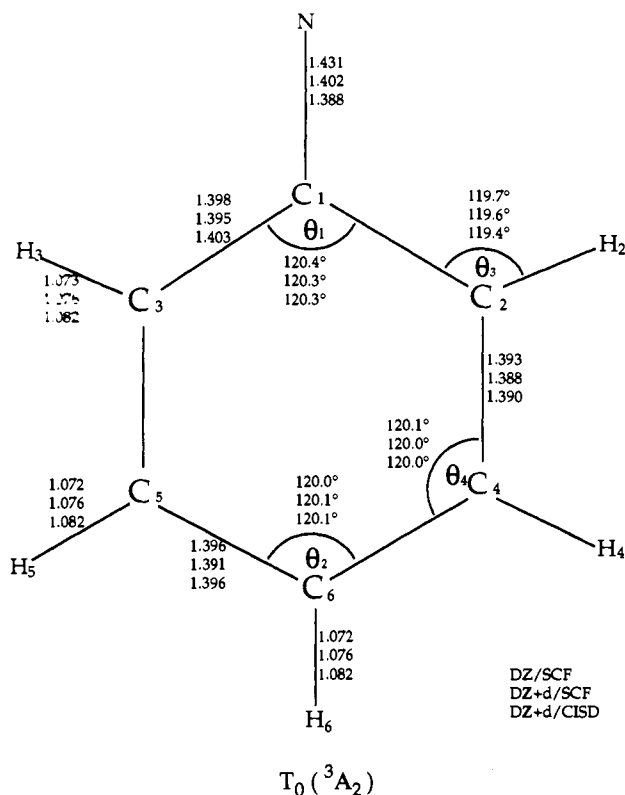
Figure 3. The equilibrium geometry for the $^3A_2$ ground state of phenylnitrene at various levels of theory. Bond lengths are in angstroms and angles in degrees.
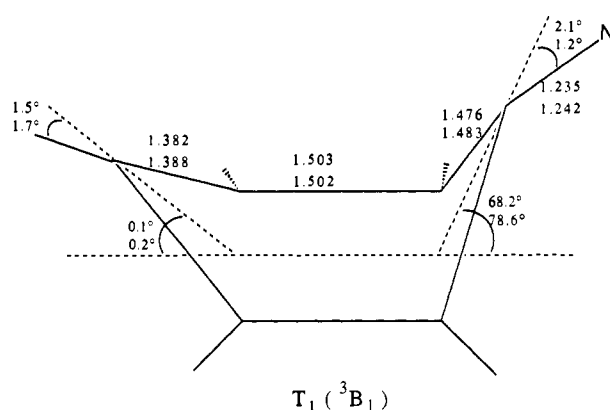

Figure 4. The puckered structure for the first excited triplet state (T_1 state, $^3B_1$ symmetry) of phenylnitrene at various levels of theory. Bond lengths are in angstroms and angles in degrees.

Table VI. Comparison of C–N Bond Lengths for PhN and Various Related Molecules

	C–N bond length (in Å)	
	expt	ab initio
C_6H_5N		1.402 (DZ+d SCF)
		1.388 (DZ+d CISD)
$C_6H_5NH_2$	1.402^a	1.415 (4-21G* HF)^b
CH_3N	1.411^c	1.440 (DZP SCF)^d
		1.442 (DZP CISD)^d
		1.424 (QZ+2p+f CISD)^d
CH_3NH_2	1.465^e	1.456 (DZP SCF)^d
		1.466 (DZP CISD)^d
		1.461 (QZ+2p+f CISD)^d

^{a}Reference 33. ^{b}Reference 32. ^{c}Reference 34. ^{d}Reference 36. ^{e}Reference 35.

Table V. Optimized Geometries for the T_0, S_0, and T_1 States of PhN at the DZ+d CISD Level and for the S_1 State at the DZ+d TCSCF Level^a

	PhN				aniline
	T_0	S_0	S_1	T_1	expt^b
C_1–N	1.388	1.274	1.367	1.242	1.402 (2)
C_1–C_2 (=C_1–C_3)	1.403	1.473	1.408	1.483	1.397 (3)
C_2–C_4 (=C_3–C_5)	1.390	1.359	1.385	1.502	1.394 (4)
C_4–C_6 (=C_5–C_6)	1.396	1.424	1.394	1.388	1.396 (2)
C_2–H_2 (=C_3–H_3)	1.082	1.081	1.075	1.083	1.082 (4)
C_4–H_4 (=C_5–H_5)	1.082	1.082	1.076	1.079	1.083 (2)
C_6–H_6	1.082	1.081	1.076	1.081	1.080 (2)
θ_1	120.3	117.5	119.2	62.9	119.4 (2)
θ_2	120.1	119.9	121.6	111.4	118.9 (1)
θ_3	119.4	117.9	118.5	115.5	119.8 (2)
θ_4	120.0	119.1	120.0	109.9	120.0 (1)

^{a}Bond lengths in angstroms, angles in degrees. C_{2v} symmetry assumed (see Figure 1 for labeling of atoms and angles). ^{b}Reference 33.

1.388 Å due to electronic correlation effects. This ordinarily nonintuitive result is due to the presence of potentially bonding molecular orbitals that are partially unoccupied in the phenylnitrene SCF wave function. The ring C–C bond distances show that correlation effects increase these predictions by 0.002–0.008 Å from SCF to CISD at the DZ+d basis set. All of the C–H bond distances in PhN consistently increase by 0.06 Å upon going from the DZ+d SCF level of theory to DZ+d CISD. The bond angles for the T_0 state of PhN are nearly the same for the SCF and CISD.

One can also see a slight bond length alternation of the C–C bond lengths in the ring. The C_1–C_2 bond is 0.007 Å longer than the experimental C–C bond length of 1.396 Å for benzene,[31] whereas the C_2–C_4 bond is 0.006 Å shorter and the C_4–C_6 bond length is the same at 1.396 Å. The DZ+d CISD value of 1.082 Å for C–H is almost the same as the C–H bond distance of 1.083 Å in benzene,[31] which means that these C–H distances are not

affected significantly by nitrogen substitution at benzene.

As shown in Table V, a comparison between the structures of PhN and aniline shows strong similarities except for the C–N bond distance. The C–N bond length of 1.388 Å in PhN is 0.027 and 0.014 Å, respectively, shorter than the theoretical value at the 4-21G* HF level[32] and the experimental measurement for aniline.[33] The C–N bond in aniline is qualitatively sp^2–sp^3, which elongates the C–N bond length as compared to the C–N bond formed in PhN by sp^2–sp overlap. For most bond lengths and angles, the differences between the DZ+d CISD PhN optimized geometry and the experimental aniline geometry are almost within the experimental uncertainty. However, aniline exhibits less bond alternation in the phenyl ring.

For the S_0 state of PhN, the bond length alternation of the ring is much more significant (see Table V). The lower vibrational frequencies for the ring puckering modes in S_0 reflect the loss of aromatic character in the phenyl ring. The C–N bond distance of 1.274 Å for the S_0 state indicates a true double bond. The short C–N bond for this state is consistent with the higher C–N stretching frequency in S_0 than for the ground state.

Figure 4 contains selected structural parameters for the T_1 $^3B_1$ state that have been optimized using the DZ+d SCF and DZ+d CISD methods. The DZ+d SCF geometry has small but significant puckering for all four angles shown, but the DZ+d CISD geometry is very flat except for the 78.6° out-of-plane angle. From the C–C ring bond distances, the unpuckered part of the ring has allylic character. The DZ+d SCF C–C bonds retain more benzene-like values in accordance with its flatter aspect. The overall amount of puckering is also consistent with the small barrier to planarity at the DZ+d SCF level changing to a large barrier for DZ+d CISD. The forms of the π_2 and π_3 orbitals in Figure 2 may be used to explain the geometry changes upon the $\pi_3 \rightarrow$ n_x transition. The π_2 orbitals are still doubly occupied; they are

(31) Cabana, A.; Bachand, J.; Giguere, J. *Can. J. Phys.* **1974**, *52*, 1949.

(32) Niu, Z.; Boggs, J. E. *J. Mol. Struct.* **1984**, *109*, 381.
(33) Lister, D. G.; Tyler, J. K.; Hog, J. H.; Larsen, N. W. *J. Mol. Struct.* **1974**, *23*, 253.

Table VII. Rotational Constants for Phenylnitrene and the Cyanocyclopentadienyl Radical

	C_6H_5N ab initio	$C_5H_4CN^a$	$C_6H_5N^b$ guess	expt^c
A''	5.716	9.266	5.696	9.600
B''	2.871	1.926	2.097	1.983
C''	1.911	1.595	1.533	1.600

^{a}Reference 37.　^{b}Estimated values based on assumed structure of PhN, ref 13.　^{c}Reference 13.

bonding in the C–C and C–N bonds, which actually show decreases in bond distance upon going from T_0 to T_1. The largest increase in bond length is for the distance C_3–C_5, where the π_3 orbital is bonding. The sharp C_2–C_1–C_3 angle involves much p bonding character, so the C–N bond has more s character, which also contributes to the short C–N distance.

Table VI gives the experimental and theoretical C–N bond lengths for several related molecules. The sp² hybridization of carbon makes the C–N bond distance shorter in PhN and aniline as compared with sp³-hybridized carbon atoms in CH_3N^{34} and CH_3NH_2.[35] Note that the DZ+d CISD level of theory is occasionally not sufficient for reliable geometries for molecules. In the case of CH_3N, the C–N bond distance decreases by 0.018 Å at very high levels of theory (CISD with a basis set of quadrupole zeta plus double polarization plus f function quality on the C and N atoms), and is in better agreement with experiment.[36] Methylnitrene is well known to be pathological in this regard, however. The DZP CISD level of theory reproduces the C–N distance quite well for CH_3NH_2. PhN appears to be quite different from CH_3N in its behavior as different levels of theory are utilized, so it is hoped that DZ+d CISD will give a reasonably accurate description of the T_0 state of PhN.

In Table VII, the theoretical rotational constants for the ground state of PhN are compared with those from experimental paper of Cullin et al.[13] They calculated the rotational constants of PhN based on an assumed structure of PhN (a benzene ring plus an optimized C–N distance) for comparison with the results of their rotational analysis of the gas-phase spectrum at 368 nm. They found that there was poor agreement between their calculated values for PhN and their experimental results. However, their calculated rotational constants for C_5H_4CN (also based on an assumed structure) are rather close to their experimental values. This is one important reason why they concluded that the carrier of the 368-nm band in the gas phase is not phenylnitrene. The rotational constants for PhN in our quantum mechanical research are in reasonable agreement with the estimated values of Cullin et al.[13] In our research on C_5H_4CN,[37] the ab initio rotational constants match very well with the experimental rotational constants of Cullin et al.[13] Consequently, we strongly support with the primary conclusions of the Miller group.

Conclusions

The ground state of PhN is verified to be of $^3A_2$ symmetry with both unpaired electrons largely occupying nitrogen orbitals. The optimized ground-state T_0 structure strongly resembles benzene. The two lowest lying excited electronic states are predicted to be singlets, with S_0 being the open-shell singlet counterpart of T_0. The S_0 state, which is predicted to lie only 6200 cm^{-1} above T_0, has a shorter C–N distance and much more bond alternation in the benzene ring. The S_1 state is the closed-shell singlet state in which two electrons are in the n_x orbital; this state is predicted to lie 11 300 cm^{-1} above T_0 in energy.

The lowest excited triplet state ($^3B_1$) is highly puckered at low levels of theory, and higher levels of theory predict a significantly puckered structure with a substantial barrier of 8000 cm^{-1} (DZ+d CISD). The DZ+d CISD T_0–T_1 adiabatic energy difference is 18 600 cm^{-1}, whereas the remainder of the triplet excited states considered lie above 30 000 cm^{-1} at the levels of theory employed.

The available experimental vibrational frequencies of Hayes and Sheridan for PhN[8] are assigned using the theoretical ground-state T_0 frequencies. The optimized T_0 geometry gives rotational constants consistent with those empirically estimated by Cullin et al.[13] for PhN. Considering that our ab initio structure for C_5H_4CN gives rotational constants in agreement with those from the rotationally resolved experiment of Cullin et al., we support their conclusion that C_5H_4CN is the molecule responsible for the long-misidentified 368-nm gas-phase band.

(34) Carrick, P. G.; Brazier, C. R.; Bernath, P. F.; Engelking, P. C. *J. Am. Chem. Soc.* **1987**, *109*, 5100.

(35) Higginbotham, H. K.; Bartell, L. S. *J. Chem. Phys.* **1965**, *42*, 1131.

(36) Xie, Y.; Scuseria, G. E.; Yates, B. F.; Yamaguchi, Y.; Schaefer, H. F. *J. Am. Chem. Soc.* **1989**, *111*, 5181.

(37) Hamilton, T. P.; Kim, S.-J.; Schaefer, H. F. To be published.